An analytical model for the long term slag hydration kinetics in slag blended cement established from a large experimental database

Jack Atallah, François Bignonnet, Harifidy Ranaivomanana, Stéphanie Bonnet

An analytical model for the long term slag hydration kinetics in slag blended cement established from a large experimental database

Jack Atallah[a], François Bignonnet[a] Harifidy Ranaivomanana[a], Stéphanie Bonnet[a]
[a] Nantes Université, Ecole Centrale Nantes, CNRS, GeM, UMR 6183, F-44600 Saint Nazaire, France

Abstract

A model is proposed for the hydration rate of slag in slag-blended cement at long term, from 3 days up to 3 years. The model accounts for the main parameters influencing on the slag hydration kinetics: water-to-binder ratio, slag substitution level, temperature, slag Blaine fineness, proportion of reactive slag. Additionally, the chemical composition of both slag and clinker is accounted for through a new composite indicator which is the expected mass ratio of C-A-S-H produced by slag to all hydration products of slag. The model is expressed as an analytical formula based on Knudsen equation. Model parameters are first calibrated on a large experimental database of 239 points from the literature. The model is then validated on 42 independent data points. The reaction rate is shown to increase with temperature, Blaine fineness, reactive slag proportion, and water-to-binder ratio, and decrease with slag substitution level. The proposed composite chemical mass ratio is the most influential parameter. The interpretation is that the higher the amount of C-A-S-H, the slower the diffusion of ions through the forming hydrate layers, which inhibits slag hydration.

1- Introduction

Slag is a byproduct of the steelmaking industry and can be obtained from blast or electric arc furnaces. It is typically composed of silicates, aluminosilicates, and calcium-alumino-silicates[1, 2]. In recent years, the use of slag as a cementitious material has become increasingly popular due to the environmental benefits and the desire to reduce cement consumption [3]. Through incorporating slag in cement composites, a significant contribution is made to the recycling of metallic industry waste products, concurrently reducing the carbon footprint of cement production.

Slag blended cement composites have been shown to be effective in enhancing durability, particularly in applications where a low diffusion coefficient is required, such as in structures exposed to aggressive environments like marine exposure [4]. The use of slag in blended cements has been shown to improve the resistance of concrete to sulfate attack, alkali-silica reaction, and chloride penetration [5, 6].

The durability properties of these materials are strongly dependent on their hydration. Therefore, studying the kinetics of this complex process and the products formed is essential for a better understanding of the behavior of these binary binder materials.

Indeed, the hydration rate of slag is much slower than that of ordinary Portland Cement clinker due to the lower reactivity of slag compared to cement [7, 8]. The activation of slag can occur through various mechanisms. This study specifically focuses on calcic activation contributed by the portlandite formed during the hydration of the clinker. Moreover, the hydration rate of slag is influenced by several parameters including the water-to-cement ratio, temperature, chemical composition of slag and clinker, slag substitution ratio, slag fineness, and percentage of glass in the slag [9–11].

Several experimental studies by various researchers, including Escalante et al. [7], Saeki and Monteiro [12], and Bougara et al. [13], have shown that slag hydration reactions consume the portlandite produced by clinker in slag blended cements. Escalante et al. [7] found that the reactivity of slag increased with an increase in temperature (T), water-to-binder ratio (w/b), and a reduction in the replacement level of slag (λ) as confirmed by the recent work of Ali-Ahmad et al. [14]. The reactivity of slag can vary significantly depending on its origin, chemical composition and processing. Therefore, accurately modeling the hydration process of slag-blended cements necessitates a comprehensive consideration of the key factors affecting slag reactivity, as well as a thorough understanding of the primary interactions between the hydration reactions of clinker and slag.

Previous studies have attempted to model slag hydration kinetics, i.e. the evolution of the slag hydration degree with time, using empirical formulas [7, 14–20]. However, these models have limitations. Some of these models have been developed to reproduce calorimetry tests and have been validated only at early age, while slag hydrates over several months [15, 18, 21]. The effect of the influencing parameters is not comprehensively accounted for. Further, these models have been calibrated and validated on limited experimental data, which may not comprehensively cover the broader spectrum of influencing parameters in slag hydration kinetics. These will be discussed in detail in the following section 2.

The objective of this study is to develop an analytical model for predicting the long term kinetics of slag hydration in blended cement composites, from one week to several years.

The article is organized as follows: first, previous research on slag-blended cement composites and the kinetics of slag hydration is reviewed. Next, the collection of the experimental database is described, followed by the development of a new slag hydration kinetic formula. Finally, the significance of the findings and their implications for further research is discussed.

2- Review of models and experiments on slag-blended cement and slag hydration kinetics

2.1- Critical review on modeling approaches

2.1.1- Experimental methods for the determination of slag hydration degree

Currently, the most commonly used method to study the hydration kinetics of cement-based materials is the determination of the isothermal hydration heat emission curve of the material. This curve informs on the overall rate and degree of hydration of the cement and the blended mineral admixtures. Calorimetry provides valuable insights into early-age cement hydration (up to 28 days) and allows for the development of models to estimate the hydration degree evolution by analyzing heat release curves. However, it's essential to acknowledge that a model effective at early stages may not necessarily maintain accuracy over extended periods, given the slow nature of slag hydration kinetics.

Alternative experimentally-based methods for predicting hydration degree exist. They are mainly based on the ratio between chemically bound water at time t and chemically bound water for a complete hydration, *i.e*, when t tends toward infinity. Different experimental procedures are proposed in the literature to estimate the amount of non-evaporable water at time t: from Loss On Ignition (LOI) measurements between 105°C and 550°C [22] or from the interpretation of the endothermic peaks on the differential thermogravimetric analysis results as suggested by different authors[14, 23, 24]. The amount of chemically bound water for a complete hydration ($t=\infty$) can be estimated from analytical equations [23–25] but could also be determined from geochemical modeling according to [21]. It is worth noting that the hydration degree values strongly depend on the method of determination of chemically bound water. The later may be underestimated in the

case of LOI measurements due to the fact that samples are initially dried at 105°C until a constant mass is reached. As consequence, destabilization of ettringite and part of CSH phase probably occurs. Thus, hydration degrees obtained from one specific method may show discrepancies compared to those provided by another one.

The measurement of hydration degree can also be achieved using image analysis technique. A scanning electron-point counting procedure has been used by [26] to estimate the hydration degree of mineral additions such as fly ash or slag. The authors found that the results were comparable to those obtained using a selective dissolution method. Finally, Nuclear Magnetic Resonance (NMR) experiments are increasingly used to estimate the hydration degree of cementitious materials. For instance, Stephant [21] used ^{29}Si MAS NMR to determine separately the degrees of hydration of clinker and slag in slag blended cement pastes. Nevertheless, no comparison with other methods of determination of the hydration degree has been made to validate the results obtained.

In the database underpinning this study, the selective dissolution method [27] is extensively utilized by authors to quantify the hydration degree of slag-blended cementitious materials. This technique revolves around selectively dissolving the hydration products and unhydrated cement [28, 29] while leaving the anhydrous slag portion intact, based on EDTA as presented in [27]. Prior studies have disclosed multiple constraints of this method, notably concerning the partial dissolution of the hydration products [30], as well as leaving residues of certain cementitious materials and hydrated phases of slag [31, 32]. This requires the implementation of corrective adjustments to account for a margin error of ±10 % [30]. Furthermore, Goguel [33] further proved the presence of a minor percentage of undissolved cement hydration products. Based on these observations, Demoulian [34] has refined this technique and enhanced its precision and reliability in the evaluation of slag-blended cement hydration.

2.1.2- Models of hydration reactions in slag blended cement

Due to the coexistence of the slag and clinker hydration, the hydration reactions of slag blended cement are more complex than that of pure Portland cement [35]. This complexity is compounded by the fact that the reactions are interdependent, affecting each other's kinetics and products. Several models have been proposed to capture the interdependence of the reactions.

Chen and Brouwers [36] proposed a reaction model for slag-blended cements based on stoichiometry calculations which link the chemical compositions of the initial unreacted phases to the volumes of produced hydration products and the resulting C-S-H composition. This calculation was integrated with the hydration model developed by with Van Eijk [37], enabling the prediction of the microstructure development in slag-blended cement systems. Kolani [5] introduced an incremental model that relies on identifying the degrees of hydration, heat exchange, and hydric state and which is coupled to stoichiometric calculations for the description of chemical reactions. The model formulates a set of differential equations to govern the temporal evolution of these variables. Schindler and Folliard [38] proposed a general kinetics hydration model capable of predicting the heat release from cementitious materials. This model integrates the impacts of the cement's mineral composition, its fineness, the inclusion of supplementary cementitious materials, the ratios of mixture components, and the characteristics of the concrete. Tydlitát et al. [39] developed a hydration model for ternary blends of Portland cement, slag, and metakaolin that accounts for the interdependence of the hydration reactions of cement, slag, and metakaolin. The model can predict the evolution of hydration heat and the degree of hydration of the ternary blend. They used a modified form of the Powers' model [40], which considers both the nucleation and growth of hydrates. The modified model was coupled with a diffusion-based chloride binding model to predict the chloride binding capacity of the ternary blend. The model was validated using experimental data from isothermal calorimetry and chloride

binding tests. Similarly, Merzouki et al. [41] proposed a hydration model for slag cements blends that also accounts for the interdependence of the hydration reactions of cement and slag.

Recently, Ali-Ahmad et al. [14] have published a new hydration model for slag blended cements which takes both slag and clinker hydration kinetics and chemical reactions into account. The model is close to that developed by Kolani [5] with the same stoichiometric considerations for the description of chemical reactions. A simplified analytical resolution is proposed instead of the numerical one performed by Kolani, by directly defining hydration kinetic laws of clinker and slag. Moreover, the implementation of the model does not require additional experimental results such as calorimetry as input data. The input data are both material formulation and chemical compositions of clinker and slag. The model can predict the evolution with time of hydrated and anhydrous phases, of porosity and of dry density. However, the coefficients involved in the model proposed by Ali-Ahmad et al. depend only of the substitution rate of clinker by slag, and do not consider the influence of other factors such as temperature, slag fineness and proportion of reactive slag.

2.1.3- Models of hydration kinetics in slag blended cement

The hydration kinetics of slag in blended cements is often determined by subtracting the known cement hydration degree from the total hydration of the composite material. This method assumes that the cement and slag hydrate independently, without influencing each other's kinetics. While this approach simplifies the analysis and may not accurately reflect the interactive effects present in slag blended cements, it is nonetheless conventionally widely employed whether experimentally or analytically.

De Schutter [15, 42] proposed a hydration kinetics model valid for both Portland cement and blast-furnace slag cement at early age (up to 7 days), by which the heat production rate could be deducted from calorimetry tests as a function of the actual temperature and the degree of hydration. Wang et al. [18–20] presented a hydration kinetics model at early age (up to 3 days) for composite binder containing slag. Merzouki [41] also proposed a kinetics model for the first 6 days of hydration of a composite binder containing slag involving the chemical compositions of cement and slag, the fineness, the curing temperature, and the water-to-binder ratio. Krstulović et al. [17] proposed a hydration kinetics model for cement-based materials based on the measured data obtained by microcalorimetry for early age hydration (first 2 days). Additionally, Pane et al. [43] also studied the hydration kinetics of composite binder containing slag using differential thermal analysis, thermogravimetric analysis, and isothermal calorimetry. This model was employed to assess the hydration degree during the early stages of hydration up to 180 days. It relies on calorimetry results and necessitates experimental data to deduce the hydration degree. Wu [44] investigated the hydration kinetics of composite binder containing slag and Portland cement using an isothermal conductive calorimeter. The model's limitations lie in its stage-dependent kinetics and varying parameters, emphasizing the need for a comprehensive understanding and careful interpretation of the results.

In this comparative analysis, the selection of only two models (Chen & Brouwers [36] and Merzouki [41] more detailed below) from the literature for evaluation is based on their extensive application within the field of hydration kinetics research [45–47]. These models have been chosen because they represent the most prevalent and validated approaches, providing a robust benchmark against which the developed model can be assessed as shown in section (2.3).

The first retained analytical model to describe the kinetics of slag hydration in cement-based composites is the model of Chen & Brouwers [48]. The formula used to predict the slag hydration degree γ as a function of time t [days] is a modified Avrami [49] equation:

$$\gamma = \{1 - exp\left(-k_2(t - k_3)^{k_1}\right).\left(a^{sl}\lambda + b^{sl}\right) \quad (1)$$

where λ is the slag proportion, and with the calibrated parameters $k_1 = 0.46$, $k_2 = 0.12$, $k_3 = 0$, $a^{sl} = -0.36$ and $b^{sl} = 0.86$. The evolution of the degree of hydration of slag γ predicted by this model is in good agreement with experimental data used for calibration [50] for the first 365 days of hydration. A similar equation has been recently used by Ali-Ahmad [14] to describe the hydration kinetics of both clinker and slag but with coefficients values depending mainly on the slag proportion. The model's simplicity, arising from the omission of several input parameters that substantially impact hydration kinetics, potentially limits its accuracy. Additionally, the fact that it is calibrated on experimental data from a single reference may affect its applicability to situations not included in this dataset.

The second retained model is the Knudsen's model [51] adopted by Merzouki [41], and then reused by several authors such as Königsberger [8], Cui [52], Han [53], Stephant [21]. The slag hydration degree γ is calculated according to equation 2:

$$\gamma(t) = \frac{(t/\tau)^{\kappa}}{1 + (t/\tau)^{\kappa}} \quad (2)$$

where τ is the reaction characteristic time and κ is the reaction exponent. According to Merzouki [41] $\tau = ((10.4605 \times \lambda - 1.8289) \times e^{-E_a/RT})^{-1}$ and $\kappa = 1$, where λ is the slag proportion, E_a is the activation energy, R is the gas constant, and T is the absolute temperature. This model is originally calibrated for early-age hydration (up to 5 days of hydration).

To sum up, a variety of models have been developed to predict the hydration of slag-blended concrete. Each one has its own strengths and limitations. Most are calibrated on early age data from calorimetry. Further, most analytical models do not account simultaneously for all the main mixing parameters that have a significant influence on the hydration kinetics, which can limit their accuracy and applicability. Therefore, there is a need for a model that can capture these effects and provide more accurate predictions of the hydration behavior of slag-blended cements for long curing period, while remaining fast and reliable.

2.2- Construction of a database for long term slag hydration kinetics

To develop our hydration kinetics formula for the long term slag hydration in blended cement composites, a comprehensive database of slag-blended cement hydration kinetics is compiled. The database is created by collecting and compiling experimental data from different references, with the aim of gathering a wide range of experimental conditions that represent different sets of parameters. This approach ensures that the resulting kinetic formula could account for the effects of a broad range of parameters on the hydration kinetics of slag-blended cement composites.

The studies of Escalante [7], Kocaba [54], Schafer [50], and Lumley [55] are selected based on their use of consistent methods for sample preparation, curing conditions, and testing procedures. All the experimental data were acquired consistently through the application of the same selective dissolution protocol based on EDTA as described by Luke and Glasser [27]. Moreover, the parameters influencing the slag hydration kinetics are well documented in these references. The collected experimental results mainly report the slag hydration degree at different time points ranging from 3 to 365 days with few results up to 800 days.

The database covers a wide range of slag substitution rate (λ) , water to binder ratio (w/b), temperature (T), slag Blaine fineness (B), hydration time (t), reactive proportion of slag ($p_{reactive}$) as well as of chemical composition. The latter is quantified through a mass ratio (μ) of slag C-A-S-H to slag hydrates presented in appendix A. The water to binder ratio w/b ranges from 0.30 to 0.80, while the slag substitution rate ranges (λ) from 20% to 92% by weight of cement. The temperature (T) ranges from 10 °C to 50 °C, and the Blaine fineness level (B) ranges from 225 m^2/kg to 561 m^2/kg. The hydration time (t) ranges from 3 to 800 days and the proportion of reactive slag ($p_{reactive}$) from 0.53 to 1. A summary of these parameters, along with their respective minimum and maximum values, is provided in table 1 below.

Parameters	μ	T[°C]	w/b	λ	B[m2/kg]	$\rho_{reactive}$	Hydration time [d]
Min	0.498	10	0.3	0.2	225	0.535	3
Max	0.782	50	0.8	0.92	561	1	805

Table 1: Parameter Ranges of the data collected in literature

Table 2 shows the details of the studies [7], [54], [50, 55], included in the developed database, including the reference, water-to-binder ratio, slag substitution rate, temperature, cement fineness, and the number of degrees of hydration reported. The detailed data about the slag hydration degree for each composition subdivided over different time periods is presented in Appendix B.

Reference	**Series**	**Clinker**						**Slag**								**Mix and cure parameters**		
	#	**C**	**S**	**A**	**M**	$\overline{S}$	**F**	**C**	**S**	**A**	**M**	$\overline{S}$	**F**	**B[m²/kg]**	$\rho_{reactive}$	**T[°C]**	**w/b**	**λ**
Escalante [7] (used for calibration)	1	0.651	0.198	0.058	0.021	0.026	0.023	0.339	0.353	0.114	0.138	0	0.017	325*	0.97	10	0.35	0.3
	2	0.651	0.198	0.058	0.021	0.026	0.023	0.339	0.353	0.114	0.138	0	0.017	325*	0.97	30	0.35	0.3
	3	0.651	0.198	0.058	0.021	0.026	0.023	0.339	0.353	0.114	0.138	0	0.017	325*	0.97	50	0.35	0.3
	4	0.651	0.198	0.058	0.021	0.026	0.023	0.339	0.353	0.114	0.138	0	0.017	325*	0.97	30	0.5	0.3
	5	0.651	0.198	0.058	0.021	0.026	0.023	0.339	0.353	0.114	0.138	0	0.017	325*	0.97	10	0.35	0.5
	6	0.651	0.198	0.058	0.021	0.026	0.023	0.339	0.353	0.114	0.138	0	0.017	325*	0.97	30	0.35	0.5
	7	0.651	0.198	0.058	0.021	0.026	0.023	0.339	0.353	0.114	0.138	0	0.017	325*	0.97	50	0.35	0.5
	8	0.651	0.198	0.058	0.021	0.026	0.023	0.339	0.353	0.114	0.138	0	0.017	325*	0.97	10	0.5	0.3
	9	0.651	0.198	0.058	0.021	0.026	0.023	0.339	0.353	0.114	0.138	0	0.017	325*	0.97	50	0.5	0.3
	10	0.651	0.198	0.058	0.021	0.026	0.023	0.339	0.353	0.114	0.138	0	0.017	325*	0.97	10	0.5	0.5
	11	0.651	0.198	0.058	0.021	0.026	0.023	0.339	0.353	0.114	0.138	0	0.017	325*	0.97	30	0.5	0.5
	12	0.651	0.198	0.058	0.021	0.026	0.023	0.339	0.353	0.114	0.138	0	0.017	325*	0.97	50	0.5	0.5
	13	0.651	0.198	0.058	0.021	0.026	0.023	0.373	0.325	0.107	0.141	0	0.019	225*	0.535	10	0.5	0.3
	14	0.651	0.198	0.058	0.021	0.026	0.023	0.373	0.325	0.107	0.141	0	0.019	225*	0.535	30	0.5	0.3
	15	0.651	0.198	0.058	0.021	0.026	0.023	0.373	0.325	0.107	0.141	0	0.019	225*	0.535	50	0.5	0.3
	16	0.651	0.198	0.058	0.021	0.026	0.023	0.373	0.325	0.107	0.141	0	0.019	225*	0.535	10	0.5	0.5
	17	0.651	0.198	0.058	0.021	0.026	0.023	0.373	0.325	0.107	0.141	0	0.019	225*	0.535	30	0.5	0.5
	18	0.651	0.198	0.058	0.021	0.026	0.023	0.373	0.325	0.107	0.141	0	0.019	225*	0.535	50	0.5	0.5
Kocaba [54] (used for validation)	19	0.6867	0.2468	0.0211	0.0058	0.0182	0.0043	0.4159	0.3661	0.1221	0.0718	0.0063	0.0085	300*	0.995	20	0.42	0.4
	20	0.6867	0.2468	0.0211	0.0058	0.0182	0.0043	0.3248	0.346	0.1998	0.0917	0.0199	0.0047	400*	0.942	20	0.42	0.4
	21	0.6129	0.2051	0.051	0.0282	0.0278	0.0333	0.4159	0.3661	0.1221	0.0718	0.0063	0.0085	300*	0.995	20	0.42	0.4
	22	0.6129	0.2051	0.051	0.0282	0.0278	0.0333	0.3248	0.346	0.1998	0.0917	0.0199	0.0047	400*	0.942	20	0.42	0.4
	23	0.6418	0.2101	0.0463	0.0182	0.0278	0.026	0.4159	0.3661	0.1221	0.0718	0.0063	0.0085	300*	0.995	20	0.42	0.4
	24	0.6418	0.2101	0.0463	0.0182	0.0278	0.026	0.3248	0.346	0.1998	0.0917	0.0199	0.0047	400*	0.942	20	0.42	0.4
Schafer [50] (used for validation)	25	0.6583	0.2105	0.0599	0.0154	0.0088	0.0288	0.4258	0.346	0.1205	0.0028	0.0001	0.0058	349	0.95**	20	0.5	0.2
	26	0.6583	0.2105	0.0599	0.0154	0.0088	0.0288	0.4258	0.346	0.1205	0.0028	0.0001	0.0058	349	0.95**	20	0.5	0.4
	27	0.6583	0.2105	0.0599	0.0154	0.0088	0.0288	0.4258	0.346	0.1205	0.0028	0.0001	0.0058	349	0.95**	20	0.5	0.8
	28	0.6583	0.2105	0.0599	0.0154	0.0088	0.0288	0.3802	0.3037	0.161	0.1025	0.0053	0.0125	352	0.95**	20	0.5	0.4
Lumley	29	0.654	0.206	0.05	0.018	0.024	0.021	0.413	0.33	0.118	0.09	0.0013	0.016	498	0.81	20	0.4	0.6
	30	0.654	0.206	0.05	0.018	0.024	0.021	0.409	0.35	0.123	0.078	0.003	0.006	437	1	20	0.4	0.6

[55] (used for calibration)	31	0.624	0.193	0.057	0.025	0.04	0.02	0.413	0.33	0.118	0.09	0.0013	0.016	498	0.81	20	0.4	0.6
	32	0.624	0.193	0.057	0.025	0.04	0.02	0.409	0.35	0.123	0.078	0.003	0.006	437	1	20	0.4	0.6
	33	0.624	0.193	0.057	0.025	0.04	0.02	0.413	0.354	0.127	0.067	0.0014	0.003	451	0.9	20	0.4	0.6
	34	0.654	0.206	0.05	0.018	0.024	0.021	0.413	0.33	0.118	0.09	0.0013	0.016	498	0.81	20	0.4	0.5
	35	0.654	0.206	0.05	0.018	0.024	0.021	0.41	0.361	0.099	0.095	0.003	0.0079	561	0.96	20	0.4	0.5
	36	0.654	0.206	0.05	0.018	0.024	0.021	0.409	0.35	0.123	0.078	0.003	0.006	437	1	20	0.4	0.5
	37	0.654	0.206	0.05	0.018	0.024	0.021	0.413	0.354	0.127	0.067	0.0014	0.003	451	0.9	20	0.4	0.5
	38	0.636	0.198	0.058	0.028	0.023	0.034	0.413	0.33	0.118	0.09	0.0013	0.016	498	0.81	20	0.6	0.3
	39	0.636	0.198	0.058	0.028	0.023	0.034	0.413	0.354	0.127	0.067	0.0014	0.003	451	0.9	20	0.6	0.3
	40	0.649	0.199	0.064	0.012	0.029	0.022	0.404	0.336	0.134	0.083	0.0005	0.015	395	1	20	0.3	0.69
	41	0.649	0.199	0.064	0.012	0.029	0.022	0.363	0.31	0.16	0.11	0.0016	0.015	384	1	20	0.3	0.69
	42	0.649	0.199	0.064	0.012	0.029	0.022	0.4	0.368	0.112	0.077	0.0013	0.004	397	0.89	20	0.3	0.69
	43	0.654	0.206	0.05	0.018	0.024	0.021	0.413	0.33	0.118	0.09	0.0013	0.016	498	0.81	20	0.4	0.5
	44	0.654	0.206	0.05	0.018	0.024	0.021	0.413	0.33	0.118	0.09	0.0013	0.016	498	0.81	20	0.4	0.3
	45	0.654	0.206	0.05	0.018	0.024	0.021	0.413	0.33	0.118	0.09	0.0013	0.016	498	0.81	20	0.4	0.6
	46	0.654	0.206	0.05	0.018	0.024	0.021	0.413	0.354	0.127	0.067	0.0014	0.003	451	0.9	20	0.4	0.3
	47	0.654	0.206	0.05	0.018	0.024	0.021	0.413	0.354	0.127	0.067	0.0014	0.003	451	0.9	20	0.4	0.5
	48	0.654	0.206	0.05	0.018	0.024	0.021	0.413	0.354	0.127	0.067	0.0014	0.003	451	0.9	20	0.4	0.6
	49	0.654	0.206	0.05	0.018	0.024	0.021	0.409	0.35	0.123	0.078	0.003	0.006	437	1	20	0.4	0.5
	50	0.654	0.206	0.05	0.018	0.024	0.021	0.409	0.35	0.123	0.078	0.003	0.006	437	1	20	0.4	0.6
	51	0.636	0.198	0.058	0.028	0.023	0.034	0.4	0.368	0.112	0.077	0.0013	0.004	397	0.89	20	0.3	0.69
	52	0.636	0.198	0.058	0.028	0.023	0.034	0.4	0.368	0.112	0.077	0.0013	0.004	397	0.89	20	0.3	0.92
	53	0.636	0.198	0.058	0.028	0.023	0.034	0.404	0.336	0.134	0.083	0.0005	0.015	395	1	20	0.3	0.69
	54	0.636	0.198	0.058	0.028	0.023	0.034	0.404	0.336	0.134	0.083	0.0005	0.015	395	1	20	0.3	0.92
	55	0.654	0.206	0.05	0.018	0.024	0.021	0.413	0.33	0.118	0.09	0.0013	0.016	498	0.81	20	0.8	0.6
	56	0.654	0.206	0.05	0.018	0.024	0.021	0.413	0.33	0.118	0.09	0.0013	0.016	498	0.81	20	0.6	0.6
	57	0.654	0.206	0.05	0.018	0.024	0.021	0.413	0.33	0.118	0.09	0.0013	0.016	498	0.81	20	0.4	0.6
	58	0.654	0.206	0.05	0.018	0.024	0.021	0.413	0.354	0.127	0.067	0.0014	0.003	451	0.9	20	0.8	0.3
	59	0.654	0.206	0.05	0.018	0.024	0.021	0.413	0.354	0.127	0.067	0.0014	0.003	451	0.9	20	0.6	0.3
	60	0.654	0.206	0.05	0.018	0.024	0.021	0.413	0.354	0.127	0.067	0.0014	0.003	451	0.9	20	0.4	0.3
	61	0.654	0.206	0.05	0.018	0.024	0.021	0.413	0.354	0.127	0.067	0.0014	0.003	451	0.9	20	0.8	0.6
	62	0.654	0.206	0.05	0.018	0.024	0.021	0.413	0.354	0.127	0.067	0.0014	0.003	451	0.9	20	0.6	0.6
	63	0.654	0.206	0.05	0.018	0.024	0.021	0.413	0.354	0.127	0.067	0.0014	0.003	451	0.9	20	0.4	0.6

[*] *slag fineness estimated from the grain size distribution, by comparison to values provided by Lumley [55]*
[**] *slag reactive proportion assumed to 95%, an average value for recent references.*
Table 2: Material compositions and conditions of the slag hydration kinetics database. The full dataset is available in open-access at [56].

The chemical composition and full name of the oxides are found in table A-1 in appendix A.

2.3- Assessment of some existing hydration kinetics models against the experimental database

To highlight the importance of using a new model, a selection of existing models widely used in the literature for predicting the hydration kinetics of slag blended cement composites (Merzouki[41], Chen and Brouwers [57], VCCTL [58]) is confronted to the experimental database. These models are chosen are summarized in Table 3.

In addition, we investigate a basic, Avrami's type equation:

$$\gamma(t) = 1 - exp\left(-\left(\frac{t - t_0}{\tau}\right)^{\kappa}\right) \quad (3)$$

in which γ is the slag hydration degree, t is the hydration time, the parameters t_0, τ (the reaction characteristic time) and κ (the reaction exponent) are constants independent of the influencing variables such as temperature, slag substitution, water over binder ratio and others. These parameters are adjusted by a least square method on the experimental database presented in section 2.2, which gives t_0 = 3.07 days, τ = 1025 days and κ = 0.281.

Name	Reference	Model category	Equation number	Input parameters	Theoretical background	Domain used for calibration and validation
Merzouki	[41]	Analytical	(2)	T,λ	Knudsen	0 - 5 days
Chen & Brouwers	[57]	Analytical	(1)	λ	Avrami	28 - 365 days
VCCTL	[58]	Numerical	-	$T, \lambda, w/b$	CEMHYD3D	Early age and long-term

Table 3: Selection of existing slag hydration kinetics models from literature

The predictions generated by these models were found to be significantly different from the experimental results for the same set of parameters, as shown in Figure 1. The mismatch for Merzouki's model and VCCTL is significant for high hydration degrees, which are achieved in long term hydration studies. The R^2 values obtained from the comparison were 0.44, 0.59, 0.58 and 0.40 for Merzouki, Chen and Brouwers, Avrami and VCCTL models respectively. These low R^2 values indicates that the models presented in literature are not accurate enough to capture all factors affecting slag hydration kinetics in blended cement composites for long curing period.

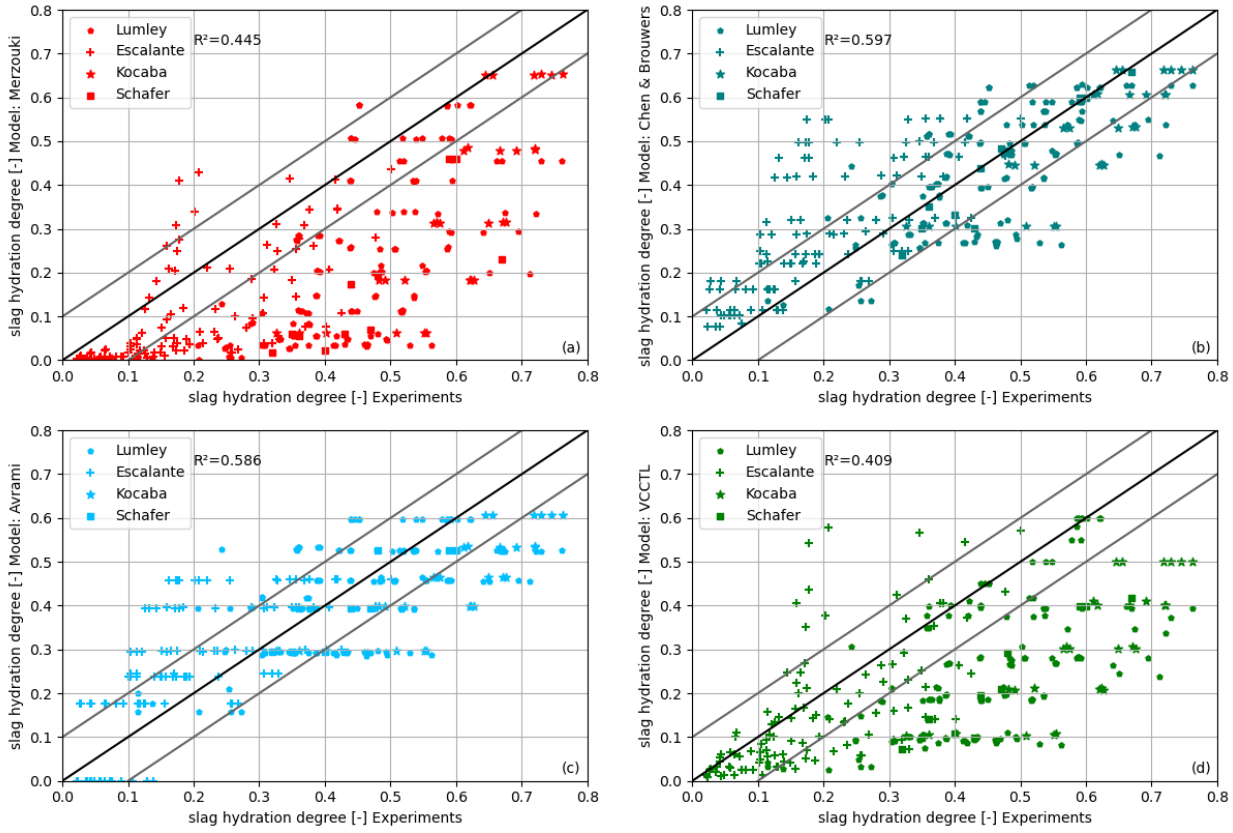

Figure 1: Validation of different models on the experimental dataset gathered.

Upon closer examination of each model, it is observed that Merzouki's model demonstrated a notable discrepancy, indicating a significant underestimation in most cases. The VCCTL model tends to underestimate the slag hydration degree as well, Conversely, Chen & Brouwers' model exhibits a comparatively more accurate estimation, yet with a large dispersion, since it does not account for several influential parameters. Similarly, Avrami's model with constant parameters includes only on time constraints and overlooks the other parameters that influences the slag hydration kinetics.

These results underscore the importance of developing a more comprehensive model of the slag hydration kinetics.

3- Modeling of slag hydration kinetics: development and validation

This section presents the development and validation of a hydration kinetics formula based on the extensive database compiled in the previous section.

3.1- Proposition of a new model for slag hydration kinetics

The development of a new hydration kinetics model for slag-blended cement hydration is based on Knudsen's equation, which is a commonly used equation for modeling the kinetics of phase transformation. Note that a similar methodology can be carried out on the basis of the Avrami equation instead. We found out that it leads to results very close to the present results based on the Knudsen equation. Since the Avrami equation requires an additional model parameter, the induction time t_0, we carry on with Knudsen's equation to reduce the number of model parameters.

The parameters that are taken into consideration include: the water to binder ratio (w/b), the slag substitution level (λ), the curing temperature (T), the chemical composition (through a mass ratio μ of slag C-A-S-H to slag hydrates detailed in appendix A), the proportion of reactive slag ($p_{reactive}$), and the Blaine fineness of slag (B).

To begin, it is essential to account for the influence of the slag inactive proportion during the hydration reactions. The reactive proportion $p_{reactive} \in [0;1]$ is the mass proportion of slag that is chemically reactive. It is identified to the vitreous fraction in slag, or reactive proportion, measured using XRD. The hydration degree of slag (γ) is thus:

$$\gamma(t) = \gamma_{reactive}(t) \times p_{reactive} \tag{4}$$

where $\gamma_{reactive}(t) \in [0;1]$ is the hydration degree of the reactive part of slag.

The kinetics of hydration of the reactive part of slag $\gamma_{reactive}(t)$ is modeled by Knudsen equation:

$$\gamma_{reactive}(t) = \frac{(t/\tau)^{\kappa}}{1 + (t/\tau)^{\kappa}} \tag{5}$$

where the reaction characteristic time τ and the reaction exponent κ are time independent functions of influencing variables. They are modeled by a separation of variable as a product of dimensionless functions C_i^{τ} and C_i^{κ} of each of the influencing variables $i \in [T, \lambda, w/b, \mu, B]$. Following a detailed assessment of different mathematical forms of functions, and their results compared to the database outlined in Table 2, the following form is retained to achieve balance between the number of model parameters and the model accuracy:

$$\tau = \tau_0 \cdot C_T^\tau \cdot C_\lambda^\tau \cdot C_{w/b}^\tau \cdot C_\mu^\tau \cdot C_B^\tau \quad (6)$$

$$\kappa = \kappa_0 \cdot C_{w/b}^\kappa \cdot C_\mu^\kappa \quad (7)$$

where the dimensionless functions C_i^τ and C_i^κ in equations (6) and (7) are defined as:

$$C_T^\tau = exp\left(\frac{E_a}{R} \times \left(\frac{1}{T} - \frac{1}{T_0}\right)\right) \quad (8)$$

$$C_B^\tau = (B/B_0)^{-1} \quad (9)$$

$$C_\lambda^\tau = \lambda^{a_\lambda} \quad (10)$$

$$C_{w/b}^\tau = (w/b)^{a_w} \quad C_{w/b}^\kappa = (w/b)^{b_w} \quad (11)$$

$$C_\mu^\tau = (1-\mu)^{a_\mu} \quad C_\mu^\kappa = (1-\mu)^{b_\mu} \quad (12)$$

where T_0 is a reference temperature set to 298 K and B_0 a reference Blaine fineness set to 450 m^2/kg.

Temperature is a critical parameter in slag hydration rate, and higher temperatures lead to faster rates. Therefore, an Arrhenius-type law on the reaction characteristic time τ is adopted in equation (8) to account for temperature effects on the hydration process. In this equation, E_a represents the activation energy, R the universal gas constant (8.3145 $J.mol^{-1}.K^{-1}$), T the temperature in Kelvin, and T_0 the reference temperature, here 298 K.

The particle size distribution of slag particles affects the available surface area for reaction, and thus plays a significant role in the overall rate of hydration. A simple model is that the reaction characteristic time τ is inversely proportional to the specific surface area, which is expressed by equation (9) in which B_0 is a reference Blaine fineness of 450 m^2/kg.

The effect of the slag substitution rate λ on the slag-blended cement hydration kinetics is modeled using a power law term on the hydration reaction characteristic time τ by equation (10). This term reflects the decrease in the rate of hydration as the substitution rate of slag increases. As more slag particles are added to the cement mixture, they replace cement particles and form a less reactive matrix.

The water-to-cement ratio is a critical parameter that influences the availability of water for the hydration reaction in slag-blended cement composites. A lower water-to-cement ratio leads to a slower hydration rate, as there is less water available for the chemical reaction to occur. This is accounted for in power law terms both on the reaction characteristic time τ and the reaction exponent κ by equation (11).

Finally, the chemical composition of the slag is also a critical parameter that affects the hydration rate. The reactivity of the slag particles depends on their chemical composition, as well as the degree to which they have reacted with the other components of the cement mixture. The chemical composition of the slag is a complex parameter that represents the different oxide compositions present in the slag. Accounting separately for each oxide proportion is cumbersome and misses chemical interactions between the oxides. To address this issue, the choice was made to express the chemical composition of the slag using a single

parameter. One effective approach is to use the ratio μ of C-A-S-H (calcium-aluminate-silicate-hydrate) formed by the slag over the total slag products that would form if all slag and clinker had reacted with water. This parameter is determined using the hydration model of Chen and Brouwers [57], as detailed in appendix A. The larger μ, the finer the porous network due to the increase in gel pores in place of capillary pores. Hence, the diffusion coefficient of ions through the hydrate layer around the hydrating slag grains is lowered, which hinders the slag reaction rate. This is accounted for by power law terms both on the reaction characteristic time τ and the reaction exponent κ by equation (12).

The values of the 8 model parameters of equations (8) to (12) are adjusted by a least square procedure on the database of Escalante [7] and Lumley [55] in table 2. The obtained correlation coefficient is R^2 = 0.805 for the subset of the database used for calibration. Optimal values of the model parameters are provided in table 4.

Model parameters					
E_a/R [K]	1491.9	τ_0 [days^{-1}]	0.014	κ_0 [-]	0.077
		a_λ [-]	0.332	b_w [-]	0.635
		a_w [-]	-3.103	b_μ [-]	-1.736
		a_μ [-]	-5.839		

Table 4: Fitted values of model parameters of equation (8) to (12) based on the fitting data from table 2.

We note that the fitted E_a/R value conforms with the values reported in literature [59–62].

3.2- Validation and illustration of the proposed slag hydration kinetics model

The model provides a more accurate representation of the slag-blended cement hydration kinetics than existing models investigated in section 2.3. We now investigate the modeled hydration rate on an independent validation subset of the database to validate the model.

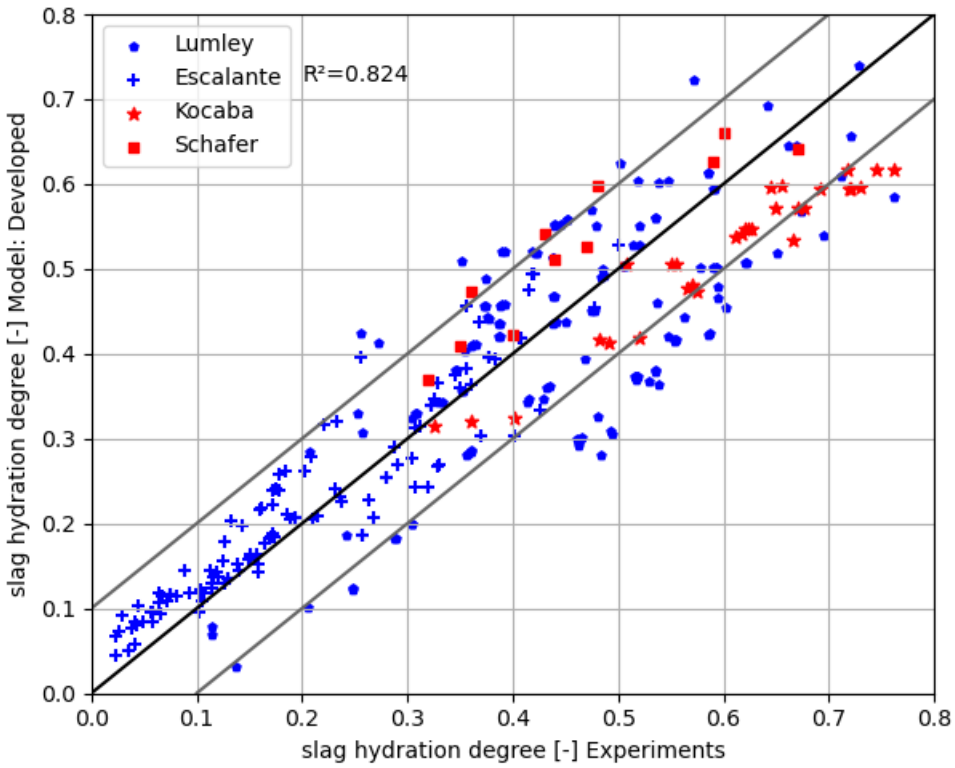

Figure 2: Validation of the developed slag hydration kinetics formula on the experimental database from table 2.

The model parameters identified from the calibration subset of the database (Escalante [7] and Lumley [55]) are used on the validation subset of the database (Kocaba [54] and Schafer[50]). Results are plotted in Figure 2, with both data used in calibration (in blue) and validation (in red). Most of the points are close to the first bisector, with few results further than the ±10% range. The correlation coefficient for the whole database, including both calibration and validation subsets, is $R^2 = 0.824$. This correlation coefficient larger than for the sole calibration subset. This is attributed to the fact that the data of Lumley [55] used in the calibration subset corresponds to very different configurations, while the validation subset is more homogeneous. This is further investigated below.

In Figure 3, the histogram displays the coefficient of determination (R^2) values for various models as applied to data subsets, categorized by authors. The hatched bars represent the dataset used for model fitting. The figure also includes a global R^2 value for the entire database. It is noteworthy that while alternative models may yield better results for the specific data subset of Schafer [50] the developed model is consistent with most data subsets. All models perform the worst with the data subset of Lumley [55] which covers a wide range of clinker and slag compositions.

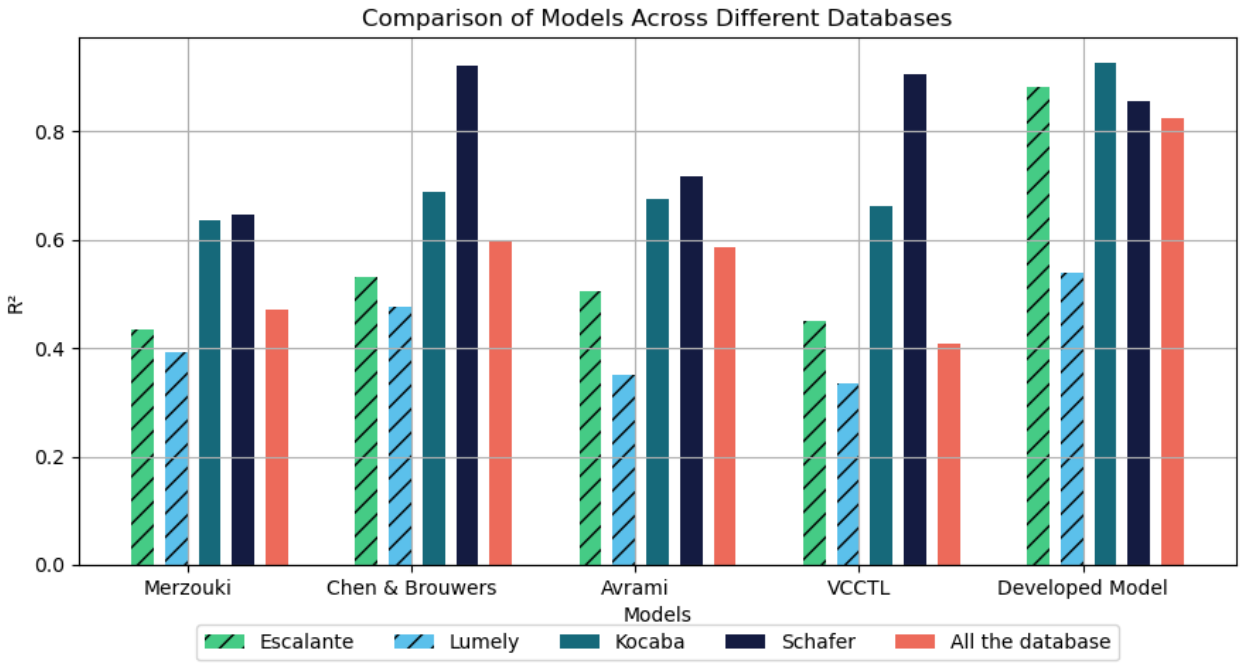

Figure 3: Comparative analysis of models' performances (R^2) across subsets of the database

In addition, Figure 4 illustrates the evolution of slag hydration kinetics over time for the mix of Escalante [7] with w/b = 0.5, λ = 0.5 and T = 10 °C, 30 °C, and 50 °C respectively (Series #10, 11 and 12 of table 2). These figures compare the present model with existing models and experimental data. As depicted in Figure 3, the developed model consistently demonstrates a superior fit to the experimental data across all conditions. Notably, it effectively captures the expected response of slag hydration kinetics to changes in temperature, aligning with experimental observations for long term hydration. Yet, the hydration kinetics at the lowest temperature (T = 10 °C) is overestimated at 90 and 180 days.

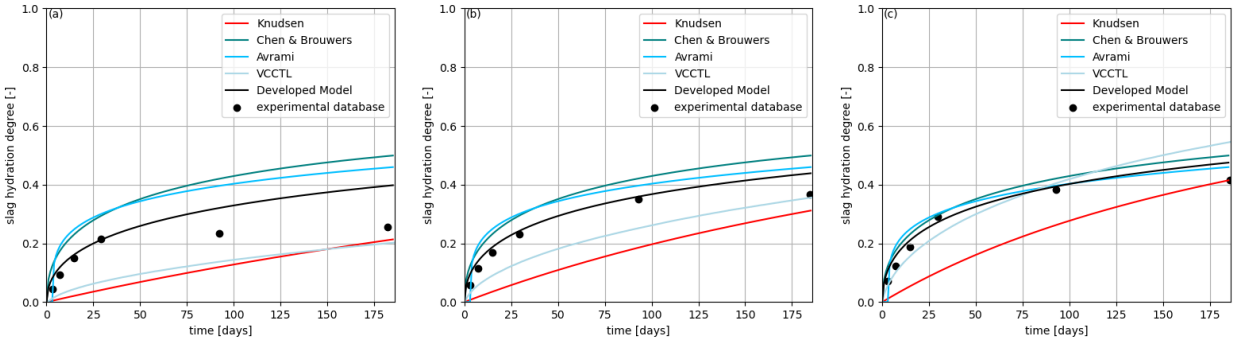

Figure 4: Models comparisons to some of the experimental results of Escalante [7] with w/b = 0.5, λ = 0.5 and T = 10 °C, 30 °C, and 50 °C respectively

3.3- Sensitivity of the developed slag hydration kinetics model to variables

In order to thoroughly investigate the influence of different variables on the performance of the developed slag kinetic model, a systematic analysis is conducted, incorporating a range of parameter values defined by the limits of the database (table 2).

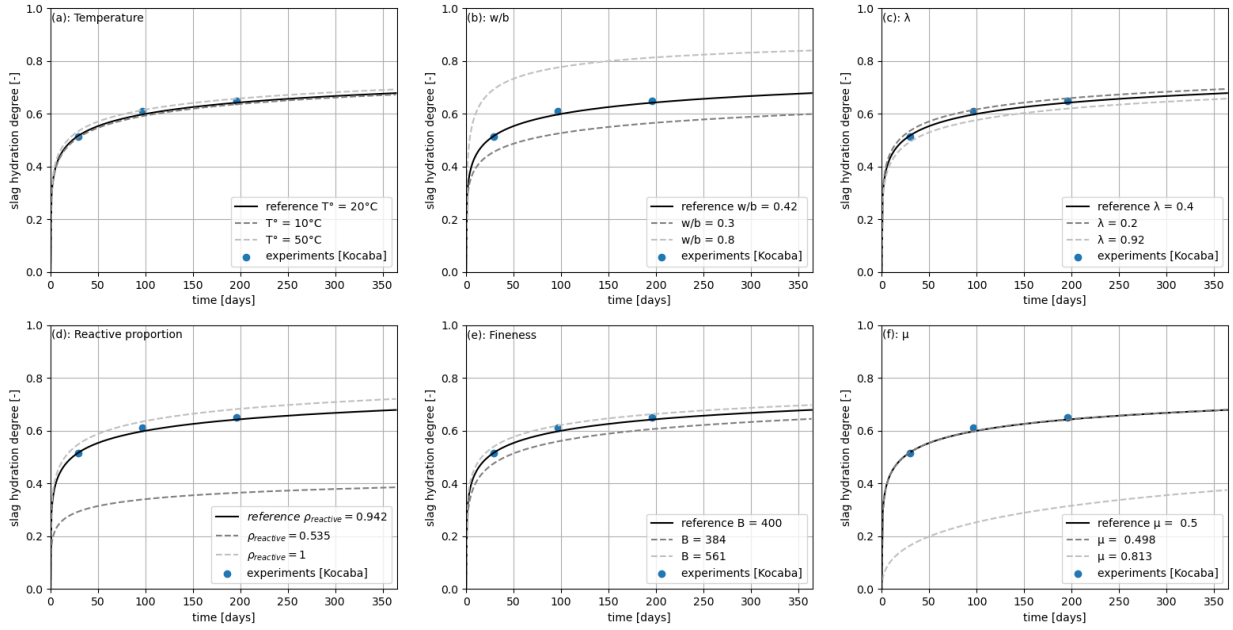

Figure 5: Influence of individual variables on slag hydration kinetics, as compared to the reference values T_{ref} = 20 °C, w/b_{ref} = 0.42, λ_{ref} = 0.4, B_{ref} = 400 m^2/kg, μ_{ref} =0.5 and $p_{reactive,ref}$ = 0.942 corresponding to experimental results of Kocaba [54] (#24 in table 2).

Figure 5 provides insight on how individual variables affect the slag hydration kinetics. In each of these figures, a single variable $i \in [T, \lambda, w/b, \mu, B, p_{reactive}]$ is changed, while keeping all other variables constant. The reference variables and experimental points correspond to the formulation of Kocaba [54] formulation with T_{ref} = 20 °C, w/b_{ref} = 0.42, λ_{ref} = 0.4, B_{ref} = 400 m^2/kg, μ_{ref} = 0.5 and $p_{reactive,ref}$ = 0.942 (#24 from table 2). This particular composition was chosen as most of its input parameters closely align with the average parameters specified in table 1. The hydration degree of the same experiment are plotted against three cases of the model, with only the selected variable $i \in [T, \lambda, w/b, \mu, B, p_{reactive}]$ taking the three values [i_{min}, i_{ref}, i_{max}] with extreme values i_{min}, i_{max} given in Table 1. The most influencing variables are the water-to-binder ratio, the proportion of reactive slag and the chemical composition ratio.

4-Conclusion

A new slag hydration kinetics model is developed to rapidly and reliably predict the time evolution of the degree of hydration of slag in slag blended cement-based materials. The model encompasses a wide range of formulations and different experimental conditions. These conditions span variations in the chemical composition of the clinker and slag, temperature, slag substitution ratio, water-to-binder ratio, slag fineness, and reactivity, providing a comprehensive and robust foundation for the developed model.

The proposed model is based on Knudsen equation, in which the reaction characteristic time and the reaction exponent are expressed as separate functions of influencing variables. Model parameters are identified on a first subset of the large database (239 data points) and the model is validated with the other subset (42 data points). Key findings of this study include:

- The model achieves a much better coefficient of determination R^2 than existing models frequently used in the literature.
- The slag reaction rate increases with temperature, Blaine fineness, the proportion of reactive slag, and water to binder ratio.

- The slag reaction rate decreases with higher clinker substitution by slag.
- The model takes into account a novel composite variable that encapsulates the chemical compositions of slag and clinker, enhancing the model's predictive capability. The larger this ratio μ is, the slower the reaction due to a slowdown of ionic exchange in the forming hydrate layers.

This work is a contribution towards a better quantification of the time evolution of the properties of slag-blended cementitious materials. In particular, it can be used in future together with a chemical hydration model to feed multiscale models of mechanical or transport properties based on mean field homogenization techniques.

Acknowledgements

This research was funded, in whole or in part, by l'Agence Nationale de la Recherche (ANR), project ANR-20-CE22-0008-01 (DEMCOM). For the purpose of open access, the author has applied a CC-BY public copyright licence to any Author Accepted Manuscript (AAM) version arising from this submission.

Data availability

The full dataset presented in table 2 is available in open-access at [56].

Appendix A : Determination of the chemical mass ratio μ using the model of Chen and Brouwers

The hydration products in slag-blended cement paste derive from both the clinker and slag hydration. Part of Portlandite (CH) produced by the clinker hydration is consumed for the slag hydration. The product the most challenging to model is C-S-H, whose composition varies depending on its calcium substitution for silicon C/S and Aluminate for silicon (A/S) ratios. The C/S ratio in C-S-H decreases with the slag substitution level in slag-blended cement, while the A/S ratio increases. The slag reaction demands additional calcium, which is provided by the CH formed by the hydration of Portland cement.

Starting with the initial oxide compositions and their proportions in the mixture, the hydration of the two main constituents is computed separately, and then combined by considering the interaction of the hydration products. A mixture of the products of both Portland cement's hydration and slag's hydration is to form. The amount of CH formed by the Portland cement hydration is strongly dependent on the slag hydration (Pietersen and Bijen, 1994 [63] ; Regourd, 1980 [64] ; Richardson and Groves, 1992 [65]).

Three models are treated by Chen and Brouwers [36, 57] , depending on the amount of CH produced by clinker that is consumed by slag. The latter influences the C/S and A/S ratios. Only the most adequate model according to Chen and Brouwers [57]is retained in this work. It corresponds to the assumption that only a part of the CH formed by clinker hydration is consumed by the slag hydration. This is supported by comparing modeled A/S and C/S ratios with experimental results provided by Richardson et al. [65],

Clinker and slag are constituted of different oxides (presented in table A-1), whose quantities vary depending on the manufacturing techniques.

	Chemical formula	Name
C	CaO	Calcium oxide, or lime
S	SiO_2	Silicon dioxide, or silica
A	Al_2O_3	Aluminum oxide, or alumina
F	Fe_2O_3	Iron oxide, or rust
T	TiO_2	Titanium dioxide, or Titania
M	MgO	Magnesium oxide, or periclase
K	K_2O	Potassium oxide
N	Na_2O	Sodium oxide
H	H_2O	Water
C	CO_2	Carbon dioxide
$\bar{S}$	SO_3	Sulfur trioxide
P	P_2O_5	Phosphorus hemi-pentoxide

Table A-5: Clinker and slag oxides and their abbreviations.

These oxides are the constituents of the four principal clinker phases: C_3S, C_2S, C_3A and C_4AF. The proprieties of the clinker phases are presented in table A-2.

Clinker Phases	Chemical Formula	Notation	Molar Mass (g/mol)	Density(g/cm3)
Tricalcium silicate	Ca_3SiO_5	C_3S	228	3.15
Dicalcium silicate	Ca_2SiO_4	C_2S	172	3.28
Tricalcium aluminate	$Ca_3Al_2O_5$	C_3A	486	3.03
Tetra-calcium aluminoferrite	$Ca_4Al_2O_{10}Fe_2$	C_4AF	270	3.73

Table A-6: Different clinker phases and properties.

According to Chen & Brouwers [57], at specified degrees of hydration, the mole number of reagents present in the mixture can be described by the formulas presented in table A-3. We define α_i as the hydration degree of clinker phases (C3S, C3A, C2S, C4AF), γ as the hydration degree of slag, and λ the substitution ratio of slag in the binder by mass.

Reagent	Clinker hydration	Slag hydration
C3S	$n_{C_3S} = n_{C_3S,0} \times \alpha_{C_3S}$	–
C3A	$n_{C_3A} = n_{C_3A,0} \times \alpha_{C_3A}$	–
C2S	$n_{C_2S} = n_{C_2S,0} \times \alpha_{C_2S}$	–
C4AF	$n_{C_4AF} = n_{C_4AF,0} \times \alpha_{C_4AF}$	–
gypsum	$n^c_{gypsum} = n_{gypsum,0} \times \alpha_{clinker}$	–
A	$n^c_A = n_{C_3A} + n_{C_4AF}$	$n^s_A = n^s_{A,0} \times \gamma$
C	$n^c_C = n_{C_3S} + 2 \times n_S + 3 \times n_A + n_F + n_{\bar{S}}$	$n^s_C = n^s_{C,0} \times \gamma$
F	$n^c_F = n_{C_4AF}$	$n^s_F = n^s_{F,0} \times \gamma$
M	$n^c_M = n_{M,0} \times \alpha_{clinker}$	$n^s_M = n^s_{M,0} \times \gamma$

S	$n_S^c = n_{C_2S} + n_{C_3S}$	$n_S^s = n_{S,0}^s \times \gamma$
$\bar{S}$	$n_{\bar{S}}^c = n_{gypsum}$	$n_{\bar{S}}^s = n_{\bar{S},0}^s \times \gamma$

Table A-7: Reagents (oxides and clinker phases) calculation formulas.

The quantity of CH produced by the hydration of clinker and consumed by the slag hydration is:

$$n_{CH,producedclinker} = 1.2 \times n_{C_3S} + 0.2 \times \left(n_{C_2S} - 2 \times n_{C_4AF}\right)$$

$$n_{CH,consumedslag} = \frac{1.8 \times n_S^s - (n_c^s - 6 \times n_{AFt}^s)}{n_{CH,producedclinker} + \left(1.8 \times n_S^s - (n_c^s - 6 \times n_{AFt}^s)\right)} \times n_{CH,producedclinker}$$

The C/S and A/S ratios are then given by:

$$C/S = \begin{cases} (C/S)_1 = \dfrac{3 \times n_{C_3S} + 2 \times n_{C_2S} + n_c^s - 6 \times n_{AFt}^s - n_{CH,producedclinker} + n_{CH,consumedslag}}{n_{C_3S} + n_{C_2S} - 2 \times n_{C_4AF} + n_S^s}; if\,(A/S)_1 < (A/S)_{max} \\ (C/S)_2 = \dfrac{1.8 \times \left(n_{C_3S} + n_{C_2S}\right) + n_c^s - 6 \times n_{AFt}^s + n_{CH,consumedslag} + 0.85 \times n_S^s - 4 \times (n_A^s - n_{HT}^s - n_{AFt}^s)}{n_{C_3S} + n_{C_2S} - 2 \times n_{C_4AF} + 1.36 \times n_S^s}; if\,(A/S)_1 > (A/S)_{max} \end{cases}$$

where

$$A/S = min\begin{Bmatrix} (A/S)_1 = (n_A^s - n_{HT}^s - n_{AFt}^s)/n_S^s \\ (A/S)_{max} = \dfrac{1 - 0.4277 \times (C/S)_1}{4.732} \end{Bmatrix}$$

The mole number of the hydration products can be then computed using equations presented in table A-4.

Products	Clinker hydration	Slag hydration
AFt	$n_{gypsum}^c/3$	$n_{\bar{S}}^s/3$
HT	$n_M^c/5$	$n_M^s/5$
AH	$n_{C_3A} - 2 \times n_{gypsum}^c/3$	$\begin{Bmatrix} 0; if\,(A/S)_1 < (A/S)_{max} \\ n_A^s - n_{HT}^s - n_{AFt}^s - n_S^s \times (A/S)_{max}; if\,(A/S)_1 > (A/S)_{max} \end{Bmatrix}$
C-S-H	$n_{C_3S} + n_{C_2S} - 2 \times n_{C_4AF}$	$-$
C-S-A-H	$-$	n_S^s
CH	$n_{CH,producedclinker} - n_{CH,consumedslag} - n_{AH}^c - n_{monoc}^c/2 + 2 \times n_{C_4AF}$	$-$
HG	n_{C_4AF}	$-$
monoc	$n_{gypsum}^c/3$	$-$

Table A-8: Hydration products calculation formulas.

Therefore, the value of μ used in the slag kinetic model is calculated by:

$$\mu = \frac{m_{CSAH}}{m_{slagproducts}}$$

Where m_{CSAH} is the calculated mass of C-S-A-H produced by the hydration at α and γ equal to 1, and $m_{slagproducts}$ is the sum of all the slag hydration products: Aft, HT, AH and C-S-A-H.

Appendix B : Slag hydration degree from literature

Series #	Time (days)	γ
1	3	6.41
1	15	17.24
1	30	23.66
1	93	30.69
1	183	32.83
2	3	7.52
2	15	19.38
2	30	28.03
2	93	32.31
2	187	37.72
3	3	8.9
3	15	23.76
3	30	30.48
3	94	36
4	3	12.93
4	8	25.76
4	15	32
4	30	37
4	94	40.69
4	188	41.93
5	3	4.84
5	8	8.14
5	15	14.01
5	30	17.4
5	94	18.43
5	184	22.09
6	3	5.66
6	7	12.56
6	15	15.04
6	30	20.96
6	94	28.78
6	186	32.6
7	3	6.44
7	7	11.84
7	15	16.99
7	30	26.36
7	94	31.15
7	187	34.6
8	3	10.66
8	7	15.65
8	15	18.64
8	30	33
8	93	35.53
8	187	35.63
9	3	13.8
9	8	26.83
9	16	32.85
9	30	42.53
9	96	47.68
9	188	50.1
10	3	4.33
10	7	9.22
10	15	14.88
10	29	21.47
10	92	23.27
10	182	25.49
11	3	5.77
11	7	11.53
11	15	16.84
11	29	23.17
11	93	34.96
11	184	36.82
12	3	7.16
12	7	12.41
12	15	18.85
12	30	29.04
12	93	38.31
12	186	41.56
13	3	2.24
13	7	2.85
13	15	10.34
13	28	11.3
13	92	13.18
13	183	17.5
14	3	3.81
14	7	4.45
14	14	11.35
14	30	15.04
14	91	17.17
14	183	20.22
15	3	5.74
15	7	6.66
15	15	15.77
15	30	16.46
15	93	17.83
15	183	20.8
16	3	2.29
16	7	2.59
16	15	10.14
16	28	10.31
16	91	12.6
16	182	16.21
17	3	3.58
17	7	4.17
17	15	10.44
17	29	12.07
17	92	14.38
17	183	17.25
18	3	4.19
18	7	6.5
18	15	11.41
18	29	15.88
18	93	15.95
18	183	17.83
19	30	40.18
19	97	52.08
19	197	57.04
19	402	61.71
19	800	65.58
20	30	55.46
20	97	62.3
20	197	67.06
20	400	71.92
20	795	74.5
21	29	32.56
21	96	49.09
21	196	57.46
21	393	66.63
21	805	72.98
22	29	50.81
22	96	62.7
22	197	67.64
22	395	72.08
22	805	76.21
23	29	36.12
23	97	48.19
23	197	56.55
23	394	61.09
23	800	64.5
24	29	55.11
24	96	62.02
24	196	64.91
24	394	69.14
24	800	71.83
25	28	40
25	91	47
25	365	67
26	28	35
26	91	44
26	365	59
27	28	32
27	91	36
27	365	48
28	28	43
28	365	60
29	28	46.06
29	91	51.8
29	196	54.81
29	364	53.71
29	728	57.83
30	28	42.95
30	91	44.96
30	196	48.58
30	364	52
30	728	54.81
31	26	46.29
31	89	51.71
31	180	55.3
31	727	59.27
32	27	41.3
32	91	43.87
32	181	48.38
32	727	53.91
33	26	30.41
33	92	35.99
33	182	38.78
33	728	43.98
34	26	49.41
34	89	53.56
34	180	58.56
34	363	59.41
34	728	62.18
35	179	48.42
35	363	53.91
35	729	60.2
36	28	43.27
36	91	47.52
36	180	50.5
36	363	53.47
36	729	58.61
37	28	32.97
37	91	38.56
37	181	43.76
37	363	43.86
37	728	45.15
38	28	46.9
38	182	69.51
38	364	76.16
39	28	38.72
39	183	58.97
39	364	66.16
40	7	25.66
40	28	34.61
40	90	37.66
40	119	37.41
40	370	42.23
40	391	39.28
41	7	27.29
41	90	35.15
42	7	11.41
42	28	24.78
42	91	28.71
42	119	30.38
42	370	35.69
42	391	35.99
43	29	49.27
43	92	53.57
43	184	58.72
43	730	62.01
44	30	48.08
44	367	59.42
45	29	46.52
45	92	51.77
45	183	55.43
45	730	58.96
46	28	35.22
46	364	51.38
47	28	33.28
47	93	38.74
47	183	43.91
47	365	43.87
47	729	45.14
48	28	30.71
48	92	36.25
48	183	38.97
48	729	43.95
49	29	43.52
49	91	47.79
49	180	50.69
49	363	53.57
49	726	58.6
50	27	41.57
50	91	44.12
50	180	48.71
50	364	47.85
50	727	51.86
51	10	11.42
51	30	24.87
51	94	28.93
51	121	30.38
51	371	35.66
51	393	36.05
52	7	13.76
52	92	20.57
52	372	24.2
53	10	25.29
53	28	34.56
53	92	37.55
53	120	37.21
53	370	42.11
53	392	38.97
54	7	20.74
54	92	25.59
55	27	56.29
55	177	71.16
55	359	72.15
56	27	52.92
56	180	65.09
56	362	67.35
57	28	46.42
57	91	51.58
57	182	55.46
57	727	59.31
58	27	41.81
58	180	64.13
58	362	72.9
59	28	38.58
59	181	59.23
59	363	66.9
60	28	35.12
60	363	52.02
61	27	37.41
61	359	57.11
62	28	35.37
62	179	47.44
62	361	50.25
63	28	30.91
63	91	36.49
63	181	39.26
63	727	44.51

Table B-1: Slag hydration degree for all mixtures found in literature at different time.

References

1. Thomas C, Rosales J, Polanco JA, Agrela F (2019) Steel slags. In: de Brito J, Agrela F (eds) New Trends in Eco-efficient and Recycled Concrete. Woodhead Publishing, pp 169–190

2. Criado M, Ke X, Provis JL, Bernal SA (2017) Alternative inorganic binders based on alkali-activated metallurgical slags. In: Savastano Junior H, Fiorelli J, dos Santos SF (eds) Sustainable and Nonconventional Construction Materials using Inorganic Bonded Fiber Composites. Woodhead Publishing, pp 185–220

3. Panesar DK (2019) Supplementary cementing materials. In: Mindess S (ed) Developments in the Formulation and Reinforcement of Concrete (Second Edition). Woodhead Publishing, pp 55–85

4. Praveenkumar TR, Vijayalakshmi MM, Meddah MS (2019) Strengths and durability performances of blended cement concrete with TiO2 nanoparticles and rice husk ash. Constr Build Mater 217:343–351. https://doi.org/10.1016/j.conbuildmat.2019.05.045

5. Kolani B, Buffo-Lacarrière L, Sellier A, et al (2012) Hydration of slag-blended cements. Cem Concr Compos 34:1009–1018. https://doi.org/10.1016/j.cemconcomp.2012.05.007

6. Sun H, Qian J, Yang Y, et al (2020) Optimization of gypsum and slag contents in blended cement containing slag. Cem Concr Compos 112:103674. https://doi.org/10.1016/j.cemconcomp.2020.103674

7. Escalante JI, Gómez LY, Johal KK, et al (2001) Reactivity of blast-furnace slag in Portland cement blends hydrated under different conditions. Cem Concr Res 31:1403–1409. https://doi.org/10.1016/S0008-8846(01)00587-7

8. Königsberger M, Carette J (2020) Validated hydration model for slag-blended cement based on calorimetry measurements. Cem Concr Res 128:105950. https://doi.org/10.1016/j.cemconres.2019.105950

9. Rahman SMA, Mahmood AH, Shaikh FUA, Sarker PK (2023) Fresh state and hydration properties of high-volume lithium slag cement composites. Mater Struct 56:91. https://doi.org/10.1617/s11527-023-02177-x

10. Wang Q, Yan P (2010) Hydration properties of basic oxygen furnace steel slag. Constr Build Mater 24:1134–1140. https://doi.org/10.1016/j.conbuildmat.2009.12.028

11. Moranville-Regourd M (1998) 11 - Cements Made From Blastfurnace Slag. In: Hewlett PC (ed) Lea's Chemistry of Cement and Concrete (Fourth Edition). Butterworth-Heinemann, Oxford, pp 637–678

12. Saeki T, Monteiro P (2005) A model to predict the amount of calcium hydroxide in concrete containing mineral admixtures. Cem Concr Res 35:1914–1921. https://doi.org/10.1016/j.cemconres.2004.11.018

13. Bougara A, Lynsdale C, Milestone NB (2010) Reactivity and performance of blastfurnace slags of differing origin. Cem Concr Compos 32:319–324. https://doi.org/10.1016/j.cemconcomp.2009.12.002

14. Ali Ahmad M, Ranaivomanana H, Bonnet S, et al (2024) Contribution to a better understanding of long-term hydration, structuration and mechanical properties of slag based cementitious materials: Experimental and modeling approaches. Constr Build Mater 411:134664. https://doi.org/10.1016/j.conbuildmat.2023.134664

15. De Schutter G (1999) Hydration and temperature development of concrete made with blast-furnace slag cement. Cem Concr Res 29:143–149. https://doi.org/10.1016/S0008-8846(98)00229-4

16. Maekawa K, Ishida T (2002) Modeling of structural performances under coupled environmental and weather actions. Mater Struct 35:591–602. https://doi.org/10.1007/BF02480352

17. Krstulović R, Dabić P (2000) A conceptual model of the cement hydration process. Cem Concr Res 30:693–698. https://doi.org/10.1016/S0008-8846(00)00231-3

18. Wang X-Y, Lee H-S (2010) Modeling the hydration of concrete incorporating fly ash or slag. Cem Concr Res 40:984–996. https://doi.org/10.1016/j.cemconres.2010.03.001

19. Wang X-Y, Lee H-S (2012) Modeling of hydration kinetics in cement based materials considering the effects of curing temperature and applied pressure. Constr Build Mater 28:1–13. https://doi.org/10.1016/j.conbuildmat.2011.08.037

20. Wang X-Y, Lee H-S, Park K-B, et al (2010) A multi-phase kinetic model to simulate hydration of slag–cement blends. Cem Concr Compos 32:468–477. https://doi.org/10.1016/j.cemconcomp.2010.03.006

21. Stephant S (2015) Etude de l'influence de l'hydratation des laitiers sur les propriétés de transfert gazeux dans les matériaux cimentaires. These de doctorat, Dijon

22. Hornain H (2007) GranduBé: grandeurs associées à la durabilité des bétons. Presses des Ponts

23. Monteagudo SM, Moragues A, Gálvez JC, et al (2014) The degree of hydration assessment of blended cement pastes by differential thermal and thermogravimetric analysis. Morphological evolution of the solid phases. Thermochim Acta 592:37–51. https://doi.org/10.1016/j.tca.2014.08.008

24. Deboucha W, Leklou N, Khelidj A, Oudjit MN (2017) Hydration development of mineral additives blended cement using thermogravimetric analysis (TGA): Methodology of calculating the degree of hydration. Constr Build Mater 146:687–701. https://doi.org/10.1016/j.conbuildmat.2017.04.132

25. Darquennes A, Espion B, Staquet S (2013) How to assess the hydration of slag cement concretes? Constr Build Mater 40:1012–1020. https://doi.org/10.1016/j.conbuildmat.2012.09.087

26. Feng X, Garboczi EJ, Bentz DP, et al (2004) Estimation of the degree of hydration of blended cement pastes by a scanning electron microscope point-counting procedure. Cem Concr Res 34:1787–1793. https://doi.org/10.1016/j.cemconres.2004.01.014

27. Luke K, Glasser FP (1987) Selective dissolution of hydrated blast furnace slag cements. Cem Concr Res 17:273–282. https://doi.org/10.1016/0008-8846(87)90110-4

28. Levelt F, Vriezen E, VONGALEN R (1982) DETERMINATION OF THE SLAG CONTENT OF BLASTFURNACE SLAG CEMENTS BY MEANS OF A SOLUTION METHOD. Zem-Kalk-Gips 35:96–99

29. Battagin A (1992) Influence of degree of hydration of slag on slag cements. Int Congr Chem Cem 9 Th III Pp 166:

30. Taylor HFW, Mohan K, Moir GK (1985) Analytical Study of Pure and Extended Portland Cement Pastes: I, Pure Portland Cement Pastes. J Am Ceram Soc 68:680–685. https://doi.org/10.1111/j.1151-2916.1985.tb10124.x

31. Luke K, Glasser FP (1988) Internal chemical evolution of the constitution of blended cements. Cem Concr Res 18:495–502. https://doi.org/10.1016/0008-8846(88)90042-7

32. Dyson HM, Richardson IG, Brough AR (2007) A Combined ^{29} Si MAS NMR and Selective Dissolution Technique for the Quantitative Evaluation of Hydrated Blast Furnace Slag Cement Blends. J Am Ceram Soc 90:598–602. https://doi.org/10.1111/j.1551-2916.2006.01431.x

33. Goguel R (1995) A new consecutive dissolution method for the analysis of slag cements. Cem Concr Aggreg 17:84–91

34. Demoulian E, Vernet C, Hawthorn F, Gourdin P (1980) Slag content determination in cements by selective dissolution. pp 151–156

35. Narmluk M, Nawa T (2011) Effect of fly ash on the kinetics of Portland cement hydration at different curing temperatures. Cem Concr Res 41:579–589. https://doi.org/10.1016/j.cemconres.2011.02.005

36. Chen W, Brouwers HJH (2007) The hydration of slag, part 1: reaction models for alkali-activated slag. J Mater Sci 42:428–443. https://doi.org/10.1007/s10853-006-0873-2

37. Eijk RJ van (2001) Hydration of cement mixtures containing contaminants: design and application of the solidified product

38. Schindler, A.K., and Folliard, K.J. (2005) Heat of hydration models for cementitious materials

39. Tydlitát V, Zákoutský J, Schmieder M, Černý R (2012) Application of large-volume calorimetry for monitoring the early-stage hydration heat development in cement-based composites as a function of w/c. Thermochim Acta 546:44–48. https://doi.org/10.1016/j.tca.2012.07.028

40. Powers TC (1961) Fundamental aspects of shrinkage of concrete. Rev Matér 79–85

41. Merzouki T, Bouasker M, Houda Khalifa NE, Mounanga P (2013) Contribution to the modeling of hydration and chemical shrinkage of slag-blended cement at early age. Constr Build Mater 44:368–380. https://doi.org/10.1016/j.conbuildmat.2013.02.022

42. De Schutter G, Taerwe L (1995) General hydration model for portland cement and blast furnace slag cement. Cem Concr Res 25:593–604. https://doi.org/10.1016/0008-8846(95)00048-H

43. Pane I, Hansen W (2005) Investigation of blended cement hydration by isothermal calorimetry and thermal analysis. Cem Concr Res 35:1155–1164. https://doi.org/10.1016/j.cemconres.2004.10.027

44. Wu WQ. Kinetics study on hydration of blast furnace slag cement (in Chinese). J Chin Ceram Soc. 1988;16:423–8:

45. Miao M, Liu Q, Zhou J, Feng J (2019) Effects of Expansive Agents on the Early Hydration Kinetics of Cementitious Binders. Materials 12:1900. https://doi.org/10.3390/ma12121900

46. Wu L, Yan B, Lei B (2012) Cement Hydration Kinetics Research Based on Center-Particles Hydration Model. Appl Mech Mater 204–208:3634–3638. https://doi.org/10.4028/www.scientific.net/AMM.204-208.3634

47. Sheng X, Xiao S, Zheng W, et al (2023) Hydration kinetics analysis of cementitious paste composites produced by binary and ternary binder materials for potential use in massive concrete structures. Case Stud Constr Mater 18:e02209. https://doi.org/10.1016/j.cscm.2023.e02209

48. Chen W, Brouwers HJH (2011) A method for predicting the alkali concentrations in pore solution of hydrated slag cement paste. J Mater Sci 46:3622–3631. https://doi.org/10.1007/s10853-011-5278-1

49. Avrami M (1939) Kinetics of Phase Change. I General Theory. J Chem Phys 7:1103–1112. https://doi.org/10.1063/1.1750380

50. Schafer E (2004) Einfluss der Reaktionen verschiedener Zementbestandteile auf den alkalihaushalt der Porenlösung des Zementsteins PhD thesis. Clausthal University of Technology

51. Knudsen T The dispersion model for hydration of portland cement I. General concepts. Cem Concr Res 14:622-630. https://doi.org/10.1016/0008-8846(84)90024-3

52. Cui X, Ni W, Ren C (2016) Early Hydration Kinetics of Cementitious Materials Containing Different Steel Slag Powder Contents. Int J Heat Technol 34:590–596. https://doi.org/10.18280/ijht.340406

53. Han F, Zhang Z, Wang D, Yan P (2015) Hydration kinetics of composite binder containing slag at different temperatures. J Therm Anal Calorim 121:815–827. https://doi.org/10.1007/s10973-015-4631-z

54. Kocaba V, Gallucci E, Scrivener KL (2012) Methods for determination of degree of reaction of slag in blended cement pastes. Cem Concr Res 42:511–525. https://doi.org/10.1016/j.cemconres.2011.11.010

55. Lumley JS, Gollop RS, Moir GK, Taylor HFW (1996) Degrees of reaction of the slag in some blends with Portland cements. Cem Concr Res 26:139–151. https://doi.org/10.1016/0008-8846(95)00190-5

56. Atallah J, Bignonnet F, Ranaivomanana H, Bonnet S (2024) Hydration degree of slag in slag blended cement. https://doi.org/10.57745/Y9VNLO

57. Chen W (2006) Hydration of slag cement: theory, modeling and application. s.n.

58. Bullard (2010) VCCTL Software. In: NIST. https://www.nist.gov/services-resources/software/vcctl-software. Accessed 9 Jun 2022

59. Ogirigbo OR, Black L (2016) Influence of slag composition and temperature on the hydration and microstructure of slag blended cements. Constr Build Mater 126:496–507. https://doi.org/10.1016/j.conbuildmat.2016.09.057

60. Moranville-Regourd M Cements Made From Blastfurnace Slag

61. Chen W, Brouwers HJH The reaction of slag in cement: theory and computer modelling

62. Snellings R, Machner A, Bolte G, et al (2022) Hydration kinetics of ternary slag-limestone cements: Impact of water to binder ratio and curing temperature. Cem Concr Res 151:106647. https://doi.org/10.1016/j.cemconres.2021.106647

63. Pietersen HS, Bijen JMJM (1994) Fly Ash and Slag Reactivity in Cements: Tem Evidence and Application of Thermodynamic Modelling. In: Goumans JJJM, van der Sloot HA, Aalbers ThG (eds) Studies in Environmental Science. Elsevier, pp 949–960

64. Regourd M, Thomassin JH, Baillif P, Touray JC (1980) Study of the early hydration of Ca3SiO5 by X-ray photoelectron spectrometry. Cem Concr Res 10:223–230. https://doi.org/10.1016/0008-8846(80)90079-4

65. Richardson IG, Groves GW (1992) Microstructure and microanalysis of hardened cement pastes involving ground granulated blast-furnace slag. J Mater Sci 27:6204–6212. https://doi.org/10.1007/BF01133772